Pergamon

Int. J. Heat Mass Transfer. Vol. 38, No. 3, pp. 463–480, 1995

0017-9310/95 $9.50+0.00

0017-9310(94)00166-9

Heat and mass transfer model building in drying with multiresponse data

C. T. KIRANOUDIS, Z. B. MAROULIS and D. MARINOS-KOURIS

Department of Chemical Engineering, National Technical University, Zografou Campus, GR-15780, Athens, Greece

(*Received* 19 *March* 1992 *and in final form* 6 *June* 1994)

Abstract—A model building technique involving the investigation of experimental drying data that comprise responses of material moisture content and temperature is presented. It is based on an iterative procedure in which an initial process mathematical model is tested for inadequacies observed in distributions of residuals produced when predicted state variables are compared to experimental data. Model parameters are estimated by maximizing their posterior density propability distribution involving both responses simultaneously. Possible tendencies in residuals reveal inadequacies of the examined model to sufficiently describe heat and mass transfer mechanisms during drying. The significance and correlation of model parameters are studied by determining their joint confidence regions. Sensitivity analysis of model parameters related to the output state responses shows which transfer mechanism prevails in the region where tendencies are observed. This is then either suitably transformed so that lumped dependencies of model parameters are taken into consideration, or completely changed into another form that might describe transport phenomena in a more efficient way. This interative model modification is further continued until any tendency in these residuals is eliminated. The procedure adopted indicates that, in the case of vegetables, mass transfer is controlled by three mechanisms which become sequentially significant with the progress of drying: convection, followed by diffusion in the solid phase, and conversion of bound into free diffused water in the last stages of drying until equilibrium is reached. Heat transfer is controlled solely by external convection, while internal conduction remains negligible.

INTRODUCTION

The effort involved in studying basic physical or chemical steps, which are the essence of most chemical engineering operations, aims at deducing or discovering a suitable process model. A mathematical model which can sufficiently describe the fundamental process phenomena is of great significance to the analysis and synthesis of the operation, as well as to process design and optimization. Based upon the available experimental information for basic process transport mechanisms and the extent of the theoretical aspects we intend to cover, we often shift from a purely stochastic model to a fully theoretical one. The former provides negligible considerations for the fundamental structural process mechanisms, putting forward expressions that could be nothing more than a functional relation, for instance a polynomial-type correlation. The latter essentially anticipates a detailed system behaviour through proper validation of process mechanisms which are evaluated independently, and is expressed through systems of coupled time- and space-dependent differential equations. In the first case we know practically nothing about the process internal structure; in the second we know practically everything.

In most cases the situation lies somewhere in-between, since most models refered to in the literature are of a predictive deterministic type. When theory accounts for the process inadequately, we are aided by a series of planned experiments in order to arrive at a working model, in the sense that it would at least account for the major theoretical aspects of the problem. Such a model contains information over certain ranges of the variables involved, by means of equations which reflect the basic features of the mechanisms and parameters which somehow lump the existing model inadequacies with respect to process variables. Clearly, it will probably fail over more extensive ranges, where effects previously neglected become important.

When trying to interpret physical mechanisms guided by technical intuition and experimentation, a methodology can often result from our efforts to emphasize and understand the individual process examined. We can benefit from our knowledge and experience so that a process model can be built up step by step, yielding more effective and rewarding results. In each step this would adequately simulate a specific behaviour of the system, when its parameters are estimated and their precision and accuracies are evaluated. Certain modeling procedures have been suggested as to what constitutes a good strategy in these model building situations. In the techniques adopted, a statistical analysis is always applied to the estimated parameters of a tentatively entertained theoretical model, in such a way as to pinpoint its inadequacies, if they exist, so that it is possible to proceed in a logical way to an appropriate modi-

NOMENCLATURE

a_W drying air relative humidity
a_{W_E} drying air relative humidity in equilibrium with material moisture content at the interface
C parameter of the GAB equation (9) representing temperature effects
C_0 parameter of equation (10)
c_{P_S} specific heat of dry solid [J kg^{-1} K^{-1}]
c_{P_W} specific heat of water [J kg^{-1} K^{-1}]
D effective moisture diffusivity [m^2 s^{-1}]
D_0 parameter of the Arrhenius-type equation (25) or (33) for moisture diffusivity [m^2 s^{-1}]
db dry basis
E_X parameter of the Arrhenius-type equation (25) for moisture diffusivity expressing material moisture content dependence [m^2 s^{-1}]
E_T parameter of the Arrhenius-type equation (25) for moisture diffusivity expressing temperature dependence [m^2 s^{-1}]
$e_{X_{ij}}$ material moisture content residual between experimental and model fitted points
$e_{T_{ij}}$ material temperature residual between experimental and model fitted points
h_H external heat transfer coefficient [W m^{-2}]
h_M external mass transfer coefficient [kg m^{-2} s^{-1}]
h_S specific enthalpy of the solid phase [J kg^{-1}]
i number of experiment
j an experimental observation for experiment i
k effective thermal conductivity [W m^{-1} K^{-1}]
K parameter of the GAB equation (9) representing temperature effects
k_1 kinetic constant for the conversion of bound to free water [s^{-1}]
k_2 kinetic constant for the conversion of free to bound water [s^{-1}]
K_0 parameter of equation (11)
M total number of experimental observations in all experiments
N total number of experiments
n_i total number of experimental observations for experiment i
R ideal gas constant [J mol^{-1} K^{-1}]
r_B rate of conversion of bound water to free water molecules [s^{-1}]
S_T mean sum of squares of material temperature residuals
S_X mean sum of squares of material moisture content residuals
S_{XT} mean sum of products of material moisture content and temperature residuals
t time [s]
T_A drying air temperature [°C]
T_S temperature of the solid phase [°C]
$T_{S_{ij,exp}}$ experimental temperature of observation j for experiment i [°C]
$T_{S_{ij,calc}}$ model-fitted temperature of observation j for experiment i [°C]
V Bayesian estimator
V_{min} Bayesian estimator for the best model fit
X_B bounded material moisture content [kg kg^{-1} db]
X_F free material moisture content [kg kg^{-1} db]
X_M parameter of the GAB equation (9) corresponding to an absorbed monolayer [kg kg^{-1} db]
X_S material moisture content [kg kg^{-1} db]
X_{SE} equilibrium material moisture content [kg kg^{-1} db]
$X_{S_{ij,exp}}$ experimental mean material moisture content of observation j for experimental i [kg kg^{-1} db]
$X_{S_{ij,calc}}$ model-fitted mean material moisture content of observation j for experiment i [kg kg^{-1} db]
Z dimensionless distance from the geometric center of the material sample.

Greek symbols

β volume shrinkage coefficient
ΔH_S heat of sorption [J kg^{-1}]
ΔH_C parameter of the GAB equation (9) representing the difference between the heat of sorption of the monolayer and the multilayer of water [J mol^{-1} K^{-1}]
ΔH_K parameter of the GAB equation (9) representing the difference between the heat of condensation of water vapor and the multilayer of water [J mol^{-1} K^{-1}]
ε porosity
μ_T mean value of material temperature residuals distribution [°C]
μ_X mean value of material moisture content residuals distribution [kg kg^{-1} db]
ρ_B bulk solid density including pores [kg m^{-3}]
ρ_{B0} parameter of equation (8) representing complete dry solid bulk density including pores [kg m^{-3}]

ρ_P	solid particle density excluding pores [kg m^{-3}]	σ_X	mean standard deviation of material moisture content residuals distribution [kg kg^{-1} db]
ρ_S	dry solid density [kg m^{-3}]	$\chi^2_{p,(1-\alpha)}$	chi-square distribution value of p degrees of freedom at probability level α.
ρ_W	water density [kg m^{-3}]		
σ_T	mean standard deviation of material temperature residuals distribution [°C]		

fication of the model. The modified model is then analysed in a similar way, and further modifications are suggested. The cycle is repeated as often as necessary in order to reach an appropriate model. In the literature, this sequential method has been applied in both one-response [1, 2] and multiresponse cases [3].

Drying processes involve complex heat and mass transfer phenomena which occur inside the material being dried [4–7]. The theoretical representation of drying data, consisting of material moisture content and temperature responses, is fundamentally a problem of heat and mass transfer under transient conditions. The result is a system of coupled non-linear partial differential equations, which represent the heat and mass balances in the solid and air phases of the systems undergoing drying [8–11]. The solution of these equations provides profiles of material moisture content and temperature that have to fit the experimental data within the experimental error. Solution and fitting of models adopted is chiefly a laborious task of numerical analysis and in many cases involves significant computational effort, as in the case of numerous experimental data and complicated estimation schemes. The resulting functional forms of models are non-linear in the unknown parameters. Furthermore, these common model parameters have to be estimated by fitting more than one response to the experimental observations simultaneously. Using multiresponse data results in smaller confidence regions for the parameter estimates, in comparison with estimating the parameters using only the data for the single response. Thus, the prediction for the response of interest will be more accurate [12].

Difficulties in the interpretation of heat and mass transfer phenomena during drying can be overcome by systematically examining model inefficiencies in order to further modify an initially inadequate model [13]. In ref. [13], an initial group of fundamental mass transfer mechanisms was presented in an appropriate form so that a mathematical model of the process was obtained. In that model, the parameters' best values were selected by fitting the experimental data using a least-squares estimator. When the overall state of residuals suggested that the model could be further improved, tendencies in residuals turned out to be a very useful aid in determining which mechanism brought about the greatest error, resulting in this way in its elimination by improving the model parameters or completely changing the process mechanism. This resulted in a combined convection and molecular diffusion scheme involving parameters that lump process variables. In this study, heat transfer is also taken into consideration so that a complete interpretation of transport phenomena is possible. Model parameters are estimated by multiresponse statistical criteria, i.e. Bayesian inference. New building tools such as determination of the joint confidence plots of model parameters, exploration of their correlation, and model sensivity to parameter deviations are introduced. Furthermore, the results produced are compared with similar ones from the literature. The model space which initially was formed by asymptotic alternatives of an initial model is now gradually enriched by introducing state of water considerations in the last stages of drying, which considerably improve the material moisture content population of residuals, and a state-independent parameter model is proposed.

HEAT AND MASS TRANSFER MECHANISMS IN POROUS MEDIA

Development of mathematical models to describe the drying of porous solids has been a topic of research in many fields for several decades. Several review articles on drying have recently been published. Keey [14] describes the historical development of drying theory. Van Brakel [15] provides a critical review of the topic of mass transfer during convective drying. Chrirife [16], Bruin and Luyben [17], Fortes and Okos [18], Holdsworth [19], Rossen and Hayakawa [20] and Van Arsdel [21] review drying theory as applied to food materials. All agree that the key characteristics of drying models include internal and external mechanisms of moisture and heat transfer, as well as structural and thermodynamic assumptions.

Typically, drying is divided into constant- and falling-rate periods. The drying rate in the former period is determined by conditions external to the material being dried, including temperature, gas velocity and gas water activity. The controlling resistance may be associated with the transfer of energy to the solid or the transfer of mass away from the solid. Mass transfer during the falling-rate period involves the diffusion of water through material pores into the drying medium. During this period, the drying rate decreases with time, and the rate of internal mass transfer typically controls the process. In porous solids, internal mass transfer may occur within the solid phase or the void spaces [17, 22]. Several mechanisms have been proposed in the drying literature, including liquid and vapor diffusion, surface diffusion, hydrodynamic or

bulk flow, and capillary flow. An excellent review of these mechanisms is given by Waananem *et al.* [23].

The measurement of sample temperature during drying will help in determining whether a process is controlled by energy or mass transfer. A sample measurement equal to the wet bulb temperature of the surrounding medium is characteristic of energy transfer control. If the sample reaches the dry bulb temperature of the drying medium, mass transfer control is suggested. In the same sense, particle size determines whether internal resistance is important for the drying conditions and materials considered. If the drying rate changes as the experimental sample size increases, this is a strong indication that diffusion within the solid phase controls mass transfer.

The deduction of an initial mathematical model to describe heat and mass transfer in a homogeneous, isotropic, porous solid, undergoing drying by contact with a flow of heated air, will be based on three assumptions, meant to represent the physical system in mathematical terms. First, the drying system can be treated, from the macroscopic point of view, as a quasi-one-phase system, so that it is possible to define effective values for mass diffusivity and thermal conductivity. Second, during drying, moisture content, vapor pressure and temperature are in thermodynamic equilibrium within the drying material, and moisture is evaporated at the interface between the solid and gas phases. Third, material temperature and moisture content gradients are considered as the only driving forces for heat and mass transfer, respectively.

The mathematical model can now be presented as a set of non-linear partial differential equations, describing the way in which heat and mass transfer are coupled in systems undergoing drying. The general form of these equations is:

$$\frac{\partial(\rho_B X_S)}{\partial t} = \nabla(\rho_B D \nabla X_S) \tag{1}$$

$$\frac{\partial(\rho_B h_S)}{\partial t} = \nabla(k \nabla T_S) \tag{2}$$

where X_S is the material moisture content, h_S is the specific enthalpy of the solid phase, D is the diffusion coefficient, k is the thermal conductivity, and ρ_B is the bulk solid density.

Heat and mass balances at the interface provide the two boundary constraints:

$$-\rho_B D \nabla X_S = h_M(a_{W_E} - a_W) \tag{3}$$

$$k \nabla T_S = h_H(T_A - T_S) - \Delta H_S h_M(a_{W_E} - a_W) \tag{4}$$

where h_H and h_M are the external heat and mass transfer coefficients at the boundary layer, T_A and a_W are the drying air temperature and relative humidity, a_{W_E} is the water activity in the gas phase, which is in equilibrium with material moisture content in the solid phase, ΔH_S is the system heat of sorption, and T_S is the temperature of the solid phase. In these equations all state variables are computed at the interface.

The proposed model involves heat and mass transfer phenomena, each one governed by internal and external mechanisms. The corresponding parameters are effective mass diffusivity and external mass transfer coefficient, for mass transfer, and effective thermal conductivity and external heat transfer coefficient, for heat transfer. The state variables of the combined drying system is material temperature and moisture content. We prefer to use material temperature as a system state variable because it is more handy to manipulate and compare when dealing with experimental measurements.

The specific enthalpy of the solid phase is considered to be a linear function of material moisture content and temperature within the range of variables studied [13]:

$$h_S = c_{P_S} T_S + X_S c_{P_W} T_S. \tag{5}$$

The apparent bulk density of the solid phase is based on the total particle volume, including pores. It is a characteristic property of the material structure and is chiefly affected by material moisture content. A compilation of equations for structural properties has recently been presented including bulk and particle density of the solid phase, as well as the corresponding porosity as a function of material moisture content. The most important properties are listed below [24]:

$$\varepsilon = 1 - \rho_B/\rho_P \tag{6}$$

$$\rho_P = \frac{1 + X_S}{1/\rho_S + 1/\rho_W} \tag{7}$$

$$\rho_B = \frac{\rho_{B0}(1 + X_S)}{1 + \beta X_S} \tag{8}$$

where ε is the porosity of the solid phase and ρ_P is the solid particle density. All structure characteristic properties can be evaluated separately by fitting the above-mentioned equations directly to experimental data obtained for each material studied [24].

The water activity in the gas phase in equilibrium with material moisture content in the solid phase is considered to be a function of material moisture content and temperature. It is given by the semi-empirical GAB equation, which can be solved inversely [25]:

$$X_{S_E} = \frac{X_M C K a_W}{(1 - K a_W)(1 - K a_W + C K a_W)} \tag{9}$$

where X_M is the material moisture content value which corresponds to an absorbed monolayer, and K and C are model parameters which account for the temperature effect. These quantities are assumed to be functions of temperature with the following form:

$$C = C_0 \exp(\Delta H_C / R T_S) \tag{10}$$

$$K = K_0 \exp(\Delta H_K / R T_S). \tag{11}$$

The heat of sorption is approximated by the water latent heat of vaporization at the same temperature and pressure as the water is evaporated.

The non-linear partial differential equations of the mathematical model calculate material moisture content and temperature as a function of position and time. The procedure adopted for their solution consists basically of discretizing the spatial variable according to the control-volume method [26]. This method is strongly based on physical considerations, not just on mathematical manipulations. A topological normal Cartesian grid is introduced that would fit any type of integration domain. The appropriate transfer function is then integrated within each cell of the grid, resulting in a system of ordinary differential equations which are subsequently integrated with respect to time using the variable-order, fully-implicit Gear method for stiff problems, implemented in the form of the subroutine DGEAR/IMSL. The stiffness of the proposed system of differential equations results from the completely different time constants of the material moisture content part with respect to the material temperature component of the system. The geometric consideration of the grid in each cubic sample was based on its spherical equivalent, that is to say, one-dimensional spherical coordinates in a spherical domain with surface area equal to the external surface area of the corresponding cube. Material moisture content and temperature in each grid node were then integrated throughout the space integration domain in order to produce the average state values for each time instant, so that it could be compared with the corresponding experimental value. This integration was performed using the method of Simpson [27].

MULTIRESPONSE PARAMETER ESTIMATION AND MODEL BUILDING

In a multiresponse process often only one response network is of some real interest, for instance to the plant operator. However, the use of parameter estimation based on multiresponse data results in joint confidence regions for model parameters with a smaller range when compared with the ones produced from estimation of only one response [12]. In this way, estimation of certain vital model parameters can be improved when aided by additional information derived from data produced by other measured responses. In this case, common model parameters should be estimated simultaneously. In parameter estimation problems, one deals with the derivation of model parameter estimates from samples of observations. The estimators used each time handle the population of residuals created when model calculations are compared with the experimental data obtained. In any case, one must choose between a great number of rival parameter estimators and forms of residuals, in order to select from among them the most appropriate set.

In the case of drying experiments, two kinds of residuals are produced. The first one is the material moisture content residuals, $e_{X_{ij}}$, and the second one is the material temperature residuals, $e_{T_{ij}}$. In all cases, we let j be an experimental observation in a set of n_i observations measured in experiment i out of a total of N such experiments carried out. The total number of experimental observations in all experiments is M. Clearly:

$$\sum_{i=1}^{N} n_i = M. \tag{12}$$

The Bayesian approach to the common parameter estimation problem is the one that produces realistic parameter estimates through a procedure which is applicable when different response variances as well as correlations among the responses occur. In this case, parameters are estimated by minimizing the following determinant:

$$V^2 = \begin{vmatrix} S_X^2 & S_{XT} \\ S_{XT} & S_T^2 \end{vmatrix} \tag{13}$$

which is equivalent to maximizing the posterior density distribution of the common parameters when a specific sample of observations has been measured. In this equation:

$$S_X^2 = \sum_{i=1}^{N} \sum_{j=1}^{n_1} e_{X_{ij}}^2 / M \tag{14}$$

$$S_T^2 = \sum_{i=1}^{N} \sum_{j=1}^{n_i} e_{T_{ij}}^2 / M \tag{15}$$

$$S_{XT} = \sum_{i=1}^{N} \sum_{j=1}^{n_i} e_{X_{ij}} e_{T_{ij}} / M \tag{16}$$

where S_X and S_T are the mean sum of the squares of material moisture content and temperature, respectively, and S_{XT} is the mean sum of the products of material moisture content and temperature residuals. Application of a parameter estimation technique demands the determination of the form of residuals constructed for the needs of the specific problem. In the majority of cases covered in the literature, the form of residuals adopted is based on the absolute difference between experimental and calculated values for each experimental point. In this study, however, the residuals adopted will be evaluated according to the relative difference between experimental and calculated values at each experimental point observed:

$$e_{X_{ij}} = (X_{S_{ij,\text{calc}}} - X_{S_{ij,\text{exp}}}) / X_{S_{ij,\text{exp}}} \tag{17}$$

$$e_{T_{ij}} = (T_{S_{ij,\text{calc}}} - T_{S_{ij,\text{exp}}}) / T_{S_{ij,\text{exp}}} \tag{18}$$

where $X_{S_{ij,\text{calc}}}$ and $T_{S_{ij,\text{calc}}}$ are the model fitted values of material moisture content and temperature that correspond to the observations $X_{S_{ij,\text{exp}}}$ and $T_{S_{ij,\text{exp}}}$. The model-fitted material moisture content and temperature values used in the evaluation of their corresponding residuals are the average values of these state variables integrated throughout the spatial coordinate. This form of residuals weighs the experimental points to be fitted in the same manner, no matter what

the magnitude of their absolute values is. When the examined response values vary considerably within the experiments, as in the case of the material moisture content of the last drying period in the drying curves, all experimental points are equally taken into consideration so that no information resulting from different orders of magnitude is lost. These experimental points are of great significance in the determination of model parameters characterizing heat and mass transfer within the solid phase [13].

The determinant of equation (13) is always positive; it is easily proved that it can be represented by a sum of squares. The original work was slightly changed, when the Jeffrey's rule with the elements of residual covariance as parameters was used, in order to obtain a non-informative prior posterior density distribution [28, 29]. These methodologies cope with rectangular or block–rectangular data structures. In the case of irregular data structures, we can either parametrize and estimate the missing values [30] or, when missing values are numerous, we can use the joint posterior distribution of model parameters and residual covariance elements [31].

The correlation and precision of estimated parameters can be examined by means of the joint confidence regions near optimum. Joint confidence regions are areas in the multidimensional parameter space where real parameter values are most probably located [32]. An approximation of these regions in the case of Bayesian estimation, and at a certain propability level α, is given by the contour for which [12]

$$V^2 = V^2_{\min} \exp\left(\chi^2_{p,(1-\alpha)}/M\right) \tag{19}$$

where p is the number of model parameters and $V_{\min}$ is the corresponding determinant value for the optimum model fitting. Studying the residuals evaluated by applying the Bayesian inference in multiresponse cases is considered useful for two basic reasons. The first reason is to check whether the assumptions made for the application of the specific analysis appear to be violated or not, and therefore to examine the consistency of the results produced. The assumptions mentioned above are the independence of residuals coming from the same population, and these populations have zero mean, constant variance and follow a joint distribution of normal shape. Thus, if our fitted model is correct, the residuals should exhibit tendencies which tend to confirm the assumptions we have made, or, at least, should not exhibit a denial of these assumptions. The second reason is to obtain additional information from the possible inadequacies and tendencies exhibited by the resulting form of the population of residuals that would eventually guide to model improvements. In this way, one could benefit from this modeling analysis in order to build or stepwise discover a more convenient model for the process examined. This can be done by successively modifying an initial inadequate model, thus enriching the experience for the process itself. The individual and joint distributions of residuals populations will give strong indications on the tendencies and inefficiencies of the model fitted to the experimental data.

Model building techniques deal with the development of methods that, under experimentation, are able to reveal the inadequacies of a given model in such a way as to suggest specific modifications, if necessary, and therefore produce a better one. This is done by iterative procedures in which the particular model is tentatively entertained and strained in various ways, over the region of application. The model parameters are estimated and the population of residuals is obtained and examined. If the model does not deny the assumptions made for its deduction, and, furthermore, produces satisfactory results, it is accepted as it is. Otherwise, the nature of the defects interacting with the experimenter's technical background can suggest changes and remedies leading to a modified model, which is chosen from a structure involving representations of heat and mass transfer rival mechanisms, descriptions of different model parameters, and evaluation of thermophysical properties. Usually model tendencies are judged with respect to process state variables. Sensitivity analysis of model parameters that represent the corresponding transfer mechanisms, as well as the testing of the significance of the parameters, leads to the evaluation of the dominant mechanism responsible for model inadequacies. Significance and correlation of parameters are implied from their joint confidence regions. Ziegel and Gorman [3] proposed an approximate correlation matrix instead of joint confidence regions, which is usually easier to compute. However, joint confidence plots of parameters are definitely preferable due to the amount of information they carry, which is superior to any other kind of information suggested by correlation matrices. The remedy of the mechanism is accomplished by lumping process variables in the corresponding parameter or by completely changing the relevant part of the mathematical model, introducing another possible mechanism. The resulting model is subsequently entertained, and submitted to a similar strained process. In this way, several mechanisms can be judged, and various rival models can be examined. The one to be chosen as the best will be inferred by the procedure carried out so far. When all mechanisms are examined, it is possible that the model can be further improved by suggesting suitable correlations for model parameters. The iterative procedure described is depicted in Fig. 1.

The regression method used for estimating the optimum model parameter values, that is to say the ones that minimize the determinant of equation (13), was based on a sequential quadratic programming algorithm implemented in the form of the subroutine E04UCF/NAG. In this algorithm, the search direction to the optimum is the solution of a quadratic programming problem. This algorithm treats bounds, linear constraints and non-linear constraints separately.

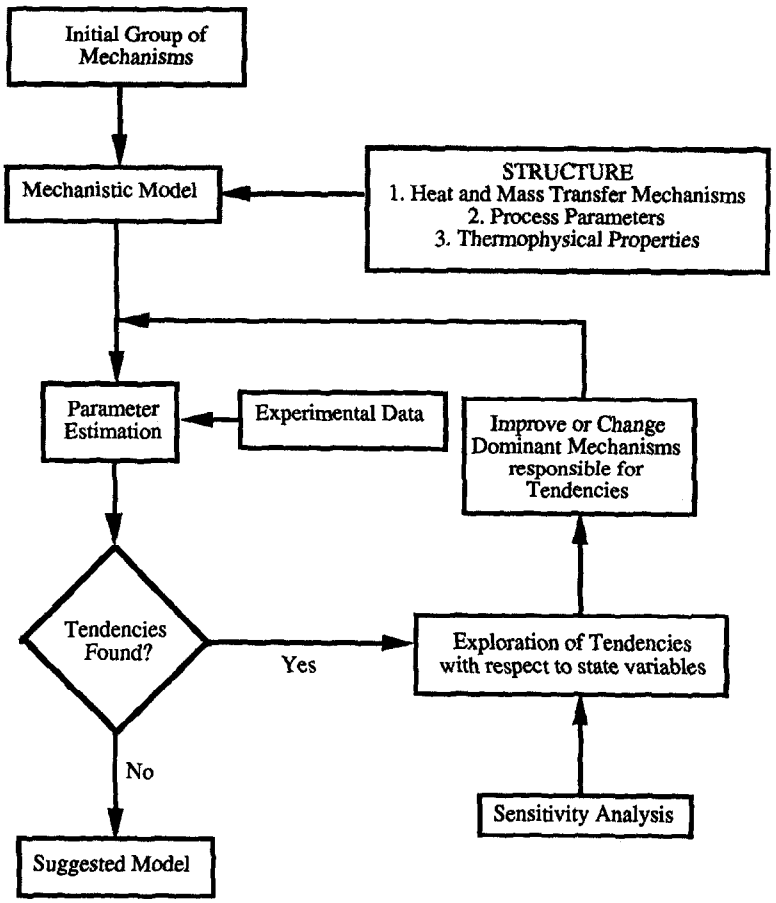

Fig. 1. Model building iterative procedure.

EXPERIMENTAL PROCEDURE

The drying experiments were conducted in a rectangular laboratory air-dryer, which consisted of an air flow rate control section, an air heating control section, an air humidifying section, and a drying test compartment where the actual drying was performed. The flow cross section was uniform throughout the dryer (20 × 20 cm). A schematic diagram of the dryer is shown in Fig. 2.

Air was circulated in the dryer by means of a centrifugal fan with controllable flow rate. The air was heated by passing through 11 heating elements of various lengths and a total of 30 kW controllable electrical power. Humidification of hot air was carried out by introducing water, in the form of liquid droplets, via a humidifing device installed in the dryer's vertical section. Air humidity in the experimental compartments could vary from 3 to 40 g kg^{-1} db.

Air velocity was measured by means of a vane anemometer sensor which produces digital pulses whose frequency was proportional to the corresponding air velocity. The pulses were read by the digital input card of an IBM PC computer. The range of measurements was 0.1–20 m s^{-1} and the sensor could resist high levels of moisture and temperature. The accuracy of measurement was 0.01 m s^{-1}. In order to avoid turbulent or twisted air flow, a flow straightener was installed at a distance of approx. 1 m in front of the anemometer. It was assembled by a number of thin-wall cylindrical tubes, approx. 1 m long, which completely filled the flow cross section.

The dry bulb temperature of the air stream was measured on-line at various spots of the dryer by means of iron–constantan thermocouples. Their analog signal was amplified 500 times, before entering the input jacks of an A/D Converter card of the PC. The cold junction temperature was measured using a thermistor-type semiconductor. The accuracy of the temperature measurement was 0.05°C. Air humidity was calculated from the dry and wet bulb temperatures measured by dry and wet thermocouples. The hot junctions of wet bulb thermocouples were covered by wicks saturated with water. The operation of wet bulb thermocouples under low air velocities was guaranteed by small fans. These fans could locally create a flow field of approx. 5 m s^{-1}, without affecting the bulk air flow. The accuracy of humidity measurement was 0.05 g kg^{-1} db.

The drying compartments of the dryer involved four square metal pans of dimension 10 × 10 cm and thick-

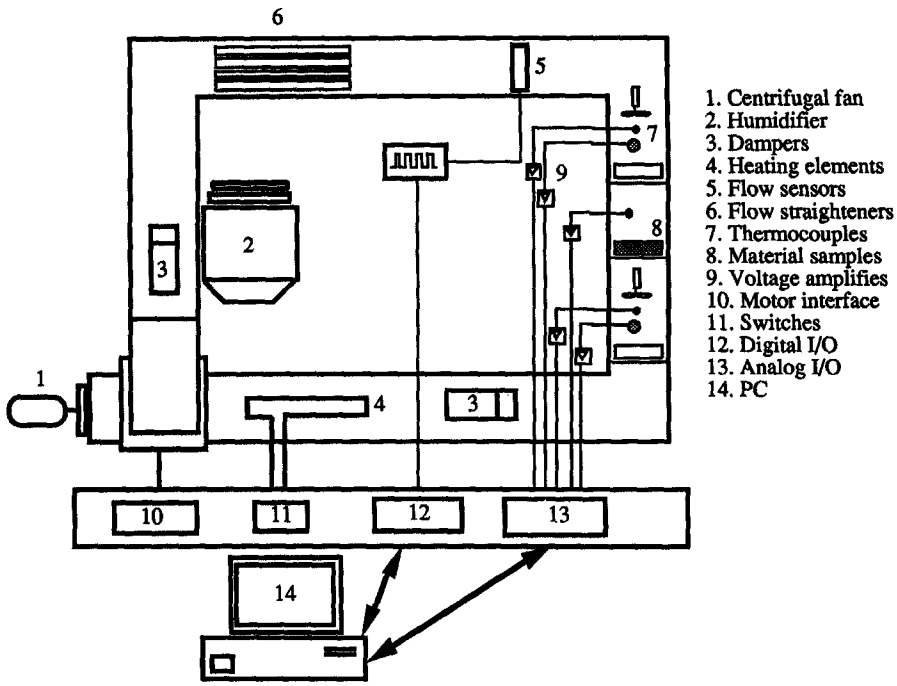

Fig. 2. Experimental laboratory dryer.

ness 5 cm, placed perpendicular to the air flow. These compartments were designed for experiments of through-type drying. The entire apparatus was insulated in order to avoid heat losses and substantial temperature differences across the test sections.

Two vegetables were used for these experiments, namely, carrot and potato. Before drying the vegetables were peeled and cut into cubes of specific size. To prevent enzymic browning, the samples were blanched for a period of 5 min in 80°C hot water. Surface water was then absorbed with filter paper. The cubes of vegetables were then uniformily distributed into identical rectangular baskets. Baskets were then placed in one of the available metal pans, in which they could fit exactly, and put in the drying compartment of the dryer. In this way, each drying experiment could involve more than one vegetable.

Air conditions throughout the experiment were measured on-line. Water losses during drying were determined off-line, by weighing each basket periodically. The average moisture content of each sample was obtained by determining the weight of the complete dry material in a vacuum drying oven. The accuracy of material moisture content measurement was 0.001 kg kg^{-1} db. The material temperature of the samples was measured on-line by means of thermocouples stuck in the bulk of certain sample cubes. An average of the measured temperatures was used for each vegetable. The accuracy of temperature measurement was 0.1°C.

Experiments to determine the influence of process variables on the drying kinetics were performed for both vegetables. The variables taken into consideration were the characteristic dimension of samples, that is to say the thickness of each cube, and the air temperature, humidity and velocity. Experiments were carried out for three cube thicknesses (5, 10 and 15 mm), at five levels of air temperature (60, 65, 70, 75 and 80°C), at three levels of air velocity (3, 4 and 5 m s^{-1}), and at air humidity levels ranging from 6 to 22 g kg^{-1} db.

A total of 100 experiments, lasting from 3 to 7 h each, were performed. They were carried out simultaneously for both vegetables, and the common air conditions for each vegetable thickness are presented in Fig. 3. In Fig. 3, the air temperature and humidity of each experiment is plotted in the psychrometric chart, for every sample thickness. Air relative

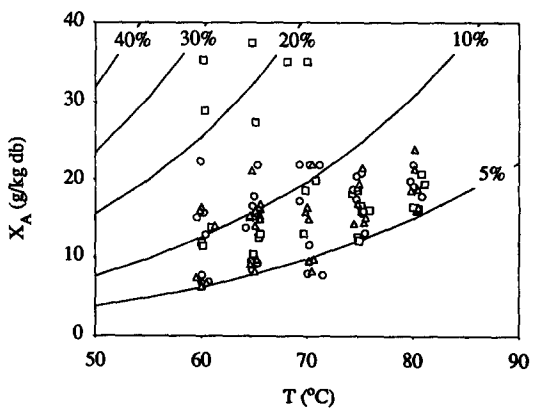

Fig. 3. Experimental space of variables: (Δ) 5 mm, (○) 10 mm, (□) 15 mm.

Table 1. Optimal Bayesian estimates for the process mathematical models developed with the sequential model building procedure

Material	h_M [kg m^{-2} s^{-1}]	h_H [W m^{-2}]	D_0 [m^2 s^{-1}]	E_X [kg kg^{-1}]	E_T [kJ mol^{-1}]	k_1 [s^{-1}]	k_2 [s^{-1}]
(1) Initial drying model							
Potato	5.45×10^{-7}	1.76×10^{-1}	2.73×10^{-9}	—	—	—	—
Carrot	6.08×10^{-7}	1.71×10^{-1}	2.18×10^{-9}	—	—	—	—
(2) Transformed diffusion coefficient drying model							
Potato	5.62×10^{-7}	1.06×10^{-1}	1.29×10^{-6}	7.25×10^{-2}	$1.70\times10^{+1}$	—	—
Carrot	5.83×10^{-7}	1.45×10^{-1}	2.71×10^{-7}	7.44×10^{-2}	$1.27\times10^{+1}$	—	—
(3) Converted bound to free water drying model							
Potato	7.47×10^{-7}	1.75×10^{-1}	6.64×10^{-7}	—	$1.55\times10^{+1}$	1.91×10^{-4}	3.43×10^{-6}
Carrot	6.93×10^{-7}	1.49×10^{-1}	1.27×10^{-6}	—	$1.70\times10^{+1}$	2.00×10^{-4}	1.70×10^{-6}

humidity contours are also included for a more comprehensive understanding of the experimental space.

RESULTS AND DISCUSSION

The Bayesian inference was applied directly to all experimental points obtained for both materials using the proposed model that accounts for both internal and external heat and mass transfer. The optimum model parameter values for heat and mass transfer coefficients are shown in Table 1. The individual residual distributions for both responses, i.e. material moisture content and temperature, along with their joint distribution for both materials, are presented in Figs. 4 and 5. In both cases, the material temperature distribution is of normal shape, with almost zero mean and adequately small standard deviation. On the other hand, the material moisture content distribution is not of normal shape, and exhibits tendencies towards negative residual values. Obviously, any effort toward model improvement should lead to the amelioration of the structure of this population. By careful inspection of the above-mentioned distribution, we notice that the two-peak curve produced suggests the existence of two different subpopulations within the first one, each one of normal shape. In our effort to detect possible tendencies with respect to the examined process variables, we introduce the plot of material moisture content residuals against their corresponding process variable values. The most revealing plot which suggested obvious tendencies was the one regarding experimental material moisture content. This plot is also included in Figs. 4 and 5. Clearly, there exist three regions of accumulation for material moisture content residuals. Residuals that constitute region A exhibit a rather dense accumulation in the neighborhood of zero, and are obviously responsible for the normal peak of the material moisture content residual distribution curve which is close to zero. Residuals of region C chiefly accumulate in an area far away from the neighborhood of zero and are obviously responsible for the normal peak of material moisture content residual distribution curve in the negative distribution axis. Residuals of region B accumulate in an area somewhere between these two extremes. We note that region A corresponds to high levels of material moisture content, that is to say in the first period of drying, while region C corresponds to low levels of material moisture content, that is to say in the last period of drying. Region B lies in-between these two periods. In conclusion, we can infer that our model predicts experimental points very well in the first period of drying, and extremely badly in its last period. Furthermore, because of the explicit negative tendency of residuals, it is clear that our model predicts higher drying rates in this period than really exist, as implied by the experimental data.

The model inadequacy is clearly due to the incapability of the transport mechanisms employed by the mathematical model used to explain why drying seems to slow down during its last period. In order to understand which transfer mechanism is to be blamed for the model behaviour throughout drying, we will study the sensitivity of model outputs with respect to its parameters, and, consequently, of the transport phenomena involved, since each of the model parameters corresponds to a transport mechanism. The drying curve predicted by the model employed, for reasonable values of model parameters and process variables, is presented in Fig. 6. Three different cases are examined. Case A corresponds to negligible mass resistance to convection, i.e. infinite value for boundary layer mass transfer coefficient. In this case mass transport is controlled by internal diffusion. Case C is the other way around. Mass transfer is controlled by convection, while diffusion is negligible, i.e. infinite value for the mass diffusion coefficient. Case B lies in-between. Both phenomena coexist and their corresponding mass transfer coefficients are significant. In all cases, heat transfer was not taken into consideration, allowing resistance to both heat transfer in the boundary layer and heat conduction to be negligible. Curve A exhibits an exponential decay as a function of time throughout drying, until the material moisture content meets its equilibrium value determined by the external medium conditions. On the other hand, curve C performs a linear decay as a function of time, expressing a constant rate throughout drying until equilibrium is again reached. The performance of curve B borrows characteristics from

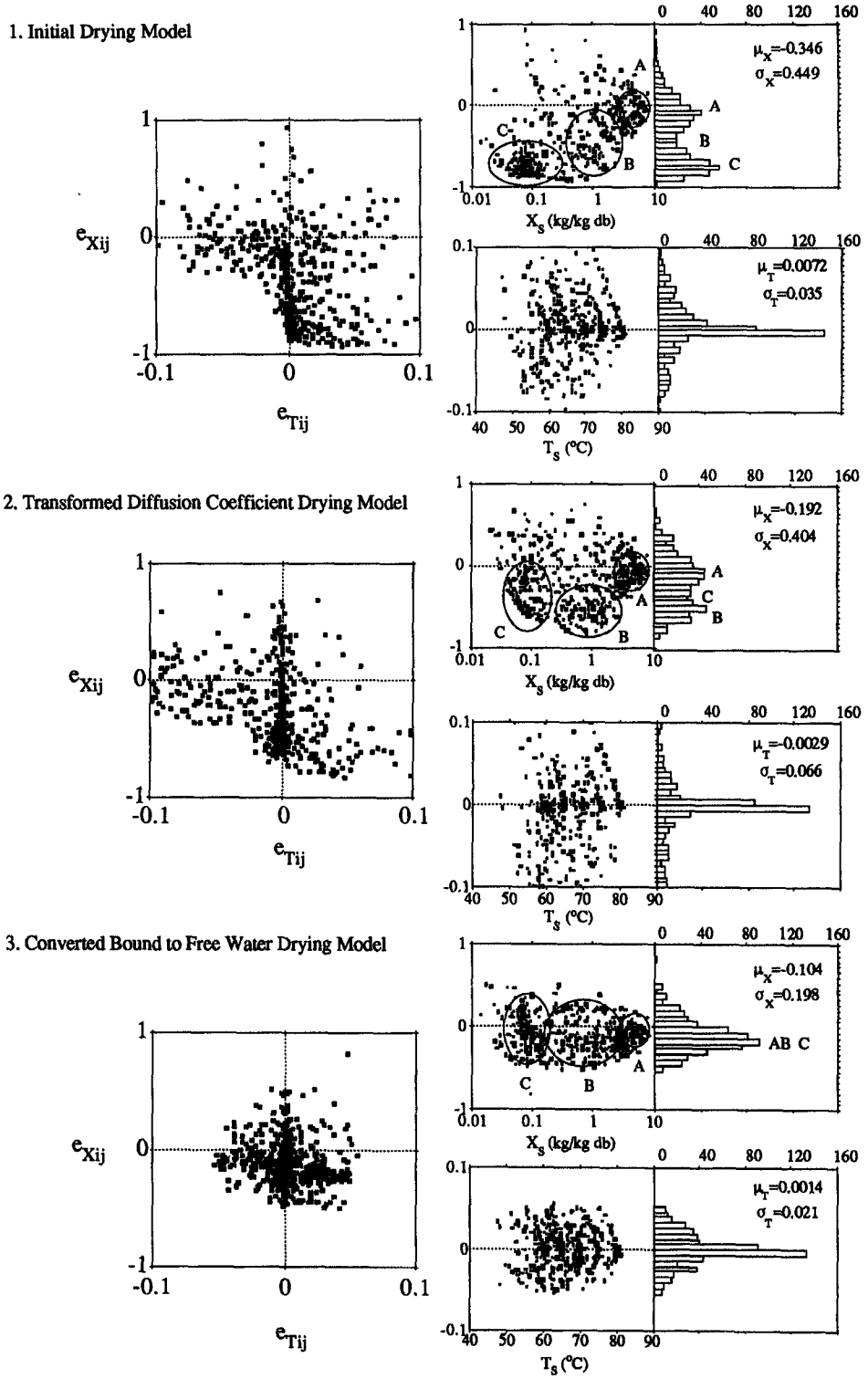

Fig. 4. Joint and individual material moisture content and temperature residual populations for carrot for all models.

both previous curves. It exhibits the linear performance of curve C in the first period of drying and the exponential performance of curve A in the last period of drying. Clearly, the total phenomenon is sequentially controlled by convection and diffusion. Convection is responsible for the first stage of drying and diffusion for the last. The performance of these curves can be explained by the form of the material

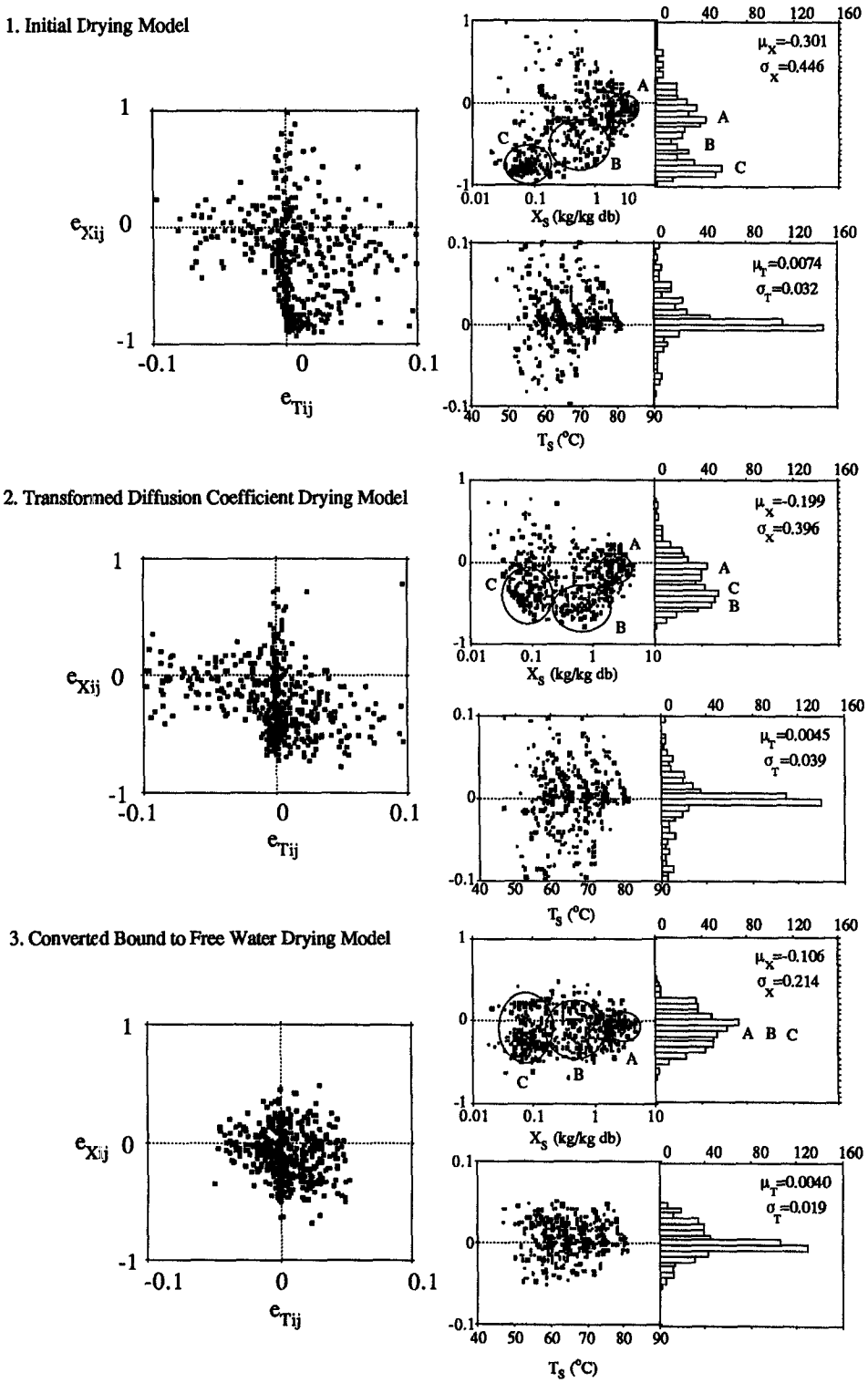

Fig. 5. Joint and individual material moisture content and temperature residual populations for potato for all models.

moisture distribution within the material studied predicted by the model. The material moisture content as a function of its dimensionless distance from the sample center and time is also presented for all cases in Fig. 6. Clearly, convection remains significant until the moisture potential at the interface becomes zero. In the case of negligible convection, the material moisture content at the interface reaches equilibrium

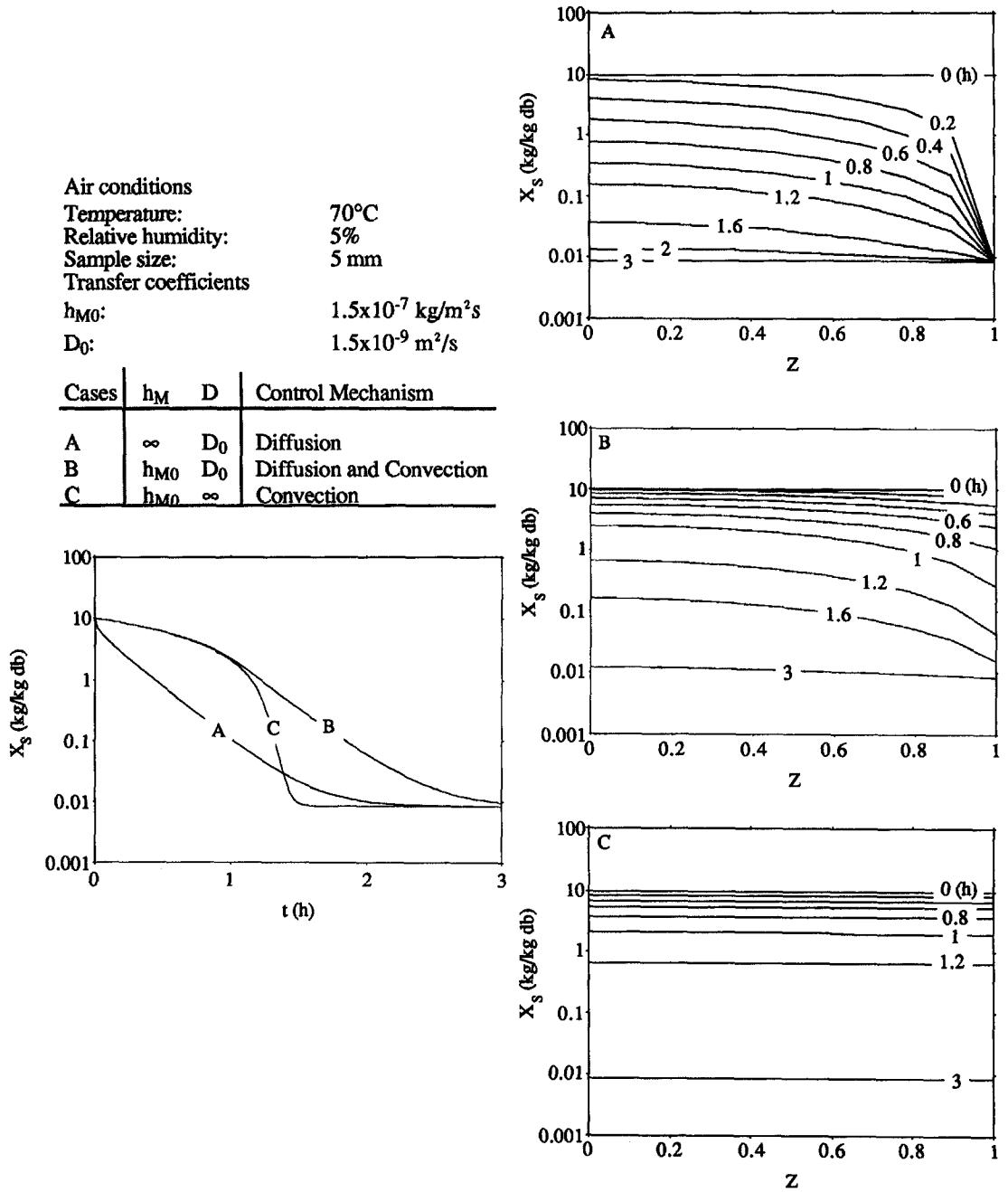

Fig. 6. Sensitivity analysis of initial drying model parameters.

immediately, whereas in the case of negligible diffusion material moisture content is uniform throughout the material dried. Similar results can be obtained if heat transfer is considered. In this case, the equilibrium temperature that will eventually be reached is the temperature of the drying medium. From the above discussion, we can infer that convection is responsible for the first stages of drying, whereas diffusion for the last. Therefore, our efforts in improving the suggested model must be focused on correcting the diffusion mechanism employed.

The significance of model parameters can be induced by plotting their joint confidence regions. These contours for a 90 and 95% level of probability are shown in Fig. 7. Obviously, we can infer that all model parameters are accurately estimated, except for the thermal conductivity of the solid phase. Joint confidence regions for mass transfer parameters are closed contours, whereas those for heat transfer parameters are contour lines parallel to the thermal conductivity axis. Practically, all positive values of effective thermal conductivity can be accepted as model estimates in

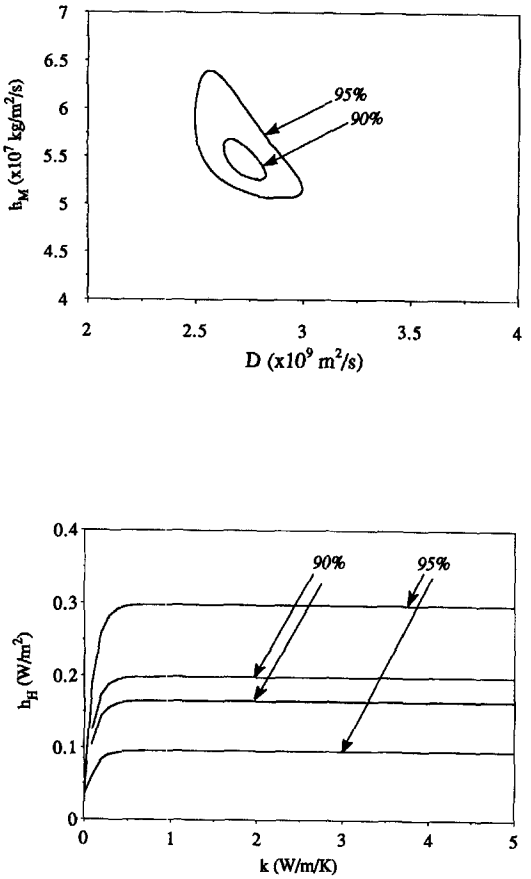

Fig. 7. Joint confidence regions of initial drying model parameters for carrot.

this particular case. This can be justified by the fact that the proposed model considers that evaporation of moisture takes place only at the interface between the solid and gas phases. Subsequently, heat conduction can contribute too little to temperature variations within the solid phase. This assumption practically dictates that the solids temperature is uniform throughout the mass of the solid. In this way, the significance of model parameters suggested that heat conduction within the solid phase can practically be ignored, thus reducing the model parameters and the participation of the corresponding phenomena studied.

From this point on, there exist two major aspects that would help improve the initial mathematical model. The first one suggests incorporation of process and state variables in model parameters resulting, in this way, in the production of effective transfer coefficients that would implicitly account for model inefficiencies and inabilities to describe the experimental data in a more sufficient way. The second one proposes that the model is suitably changed in order to take into consideration transport phenomena that can not be accurately described by the effective transport coefficient concept. In practice, the first approach is the one more frequently followed by researchers. In our case, this aspect implies correlation of external heat and mass transfer coefficients and internal effective diffusion coefficient with air condition variables and material temperature and moisture content.

External heat and mass transfer coefficients are generally considered as functions of the Reynolds number [33]. However, in our case such a correlation can not possibly be obtained due to the large superficial air velocity through samples, i.e. greater than 3 m s^{-1}, producing Reynolds number values greater than 7000 for all experimental points. This remark justifies the fact that no tendency was found for the calculated material temperature and moisture content of region A in Figs. 4 and 5 with respect to the drying air velocity. The behaviour of residuals in this region is greatly influenced by the values of external transfer coefficients, as already discussed above. Furthermore, the residuals of this region seem to perfectly accumulate near zero, producing an excellent population distribution in this area of interest. Therefore, convection heat and mass transfer will be left in the form of the initially proposed process model. What remains is to study model inadequacies with respect to the effective diffusion coefficient.

One starting point in studying the way the effective diffusion coefficient depends on process and state variables is to explore the effect of the material structure. In many cases, in porous materials, the estimated diffusion coefficient of the system corresponds to an effective moisture diffusivity, which includes the effects of moisture content, temperature and porosity. The effective diffusivity of the system is then expressed as a hybrid property which accounts for diffusion in the gas and particle phase separately, involving, in a straightforward manner, the way water is hydrodynamically diffused in each phase as well as the effect of the evolution of individual void space in the material during drying. The key variable in all structural models presented in the literature is porosity [34]. For low values of porosity, as in the first stages of drying, the effective diffusion coefficient is greatly influenced by particle diffusivity rather than by diffusion in the gas phase. For greater values of porosity, such as in the last stages of drying, diffusion in the gas phase seems to be in control. In the materials studied, the effective diffusion coefficient predicted for the last model examined is extremely small compared to the one obtained for diffusion in the gas phase [35]. Thus, although porosity does actually increase in the last period of drying, diffusion is rather controlled by the solid phase component since, if it was the other way around, drying would have accelerated rather than slowed down. In conclusion, our effort must be focused on the diffusion coefficient of the solid phase.

The most common forms of modeling the effective diffusion coefficient as a function of process and state variables involve a dependence on both material temperature and moisture content. The majority of models reported in the literature suggest that the effective mass diffusivity increases with the material moisture

content up to a certain level, which is regarded to be a function of the material temperature. The form of the mass diffusivity shape suggests that water molecules have to overcome a certain energy barrier as the material moisture content decreases, and, therefore, mass transfer slows down in the last stages of drying. Normally, moisture diffusivity is considered to be a function of temperature, usually of an Arrhenius-type dependence, something that is considered reasonable due to the increase in the molecular kinetic energy when temperature increases. The fact that the material moisture content is also included in these expressions is a defect, in the sense that we do not account for the microscopic transport phenomena directly, but is of the greatest importance if we would like to suggest an overall predictive model. In this study, the effective moisture diffusivity will be treated as a function of the material moisture content and temperature, given by the following expression [13]:

$$D = D_0 \exp(-E_X/X_S) \exp(-E_T/RT_S). \quad (20)$$

The Bayesian inference was again applied directly to all experimental points obtained for both materials using the transformed parameter model suggested above. Estimation of parameters in Arrhenius-type equations can be substantially aided when a suitable transformation takes place. This transformation produces more robust estimates of parameters [3, 36]. The optimum model parameter values for the heat and mass transfer coefficients are shown on Table 1. The variation of the effective moisture diffusivity as a function of the material moisture content and temperature is presented in Fig. 8. It is observed that an increase in its values with material moisture content takes place up to a certain level, which is a function of the material temperature. The individual residual distributions for both responses, along with their joint residual distribution for both materials are presented in Figs. 4 and 5. Again, the material temperature distribution is of normal shape, with almost zero mean and adequately small standard deviation. On the other hand, the material moisture content distribution is of normal shape but exhibits a rather high variance and, once more, tendencies towards negative residual values. Obviously, the situation is better than in the previous case. Residuals of region A remain accumulated around zero, region C has shifted considerably towards zero, but region B points remain clearly on the negative axis of residuals. What we produced is considered an improvement of the previous model but surely we have not so far explained adequately the phenomenon nor produced really satisfactory results, i.e. substantially shifted the material moisture content residuals toward zero.

Since the lumping process of state variables into model parameters did not efficiently improve the behavior of material moisture content residuals, we are forced to examine other possible transfer mechanisms that might occur during drying from the microscopic point of view. Recently, Xiong *et al.* [37] came

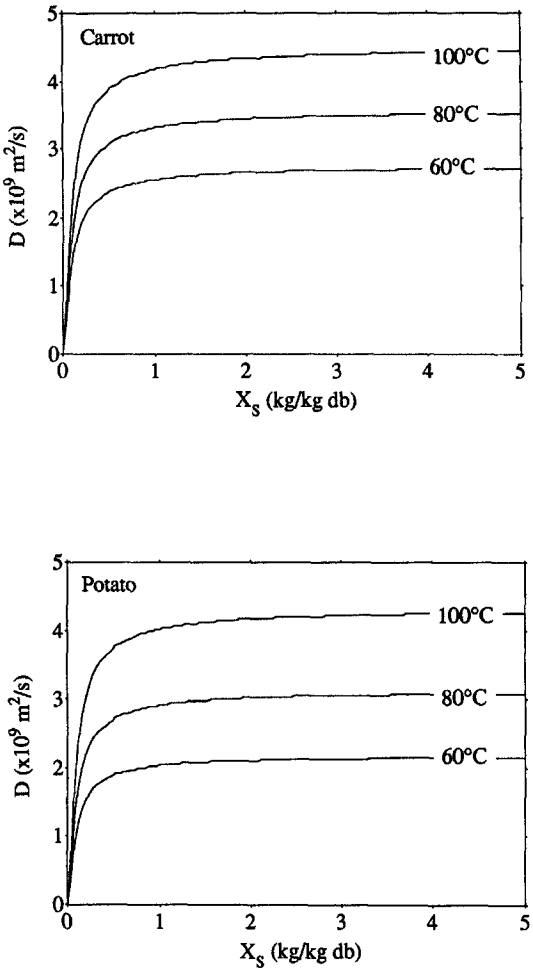

Fig. 8. Proposed dependence of material moisture content on effective diffusion coefficient for the transformed diffusion coefficient drying model.

up with a postulation that the tremendous decrease in drying rate in the last period of drying may be thought of as a result of the decrease in the availability of water molecules. Water molecules that reside in the close neighbourhood of material molecules are strongly connected to them, and the amount of energy to be overcome is proportional to the strength of these bonds. On the other hand, remote water molecules are very loosely connected with material molecules, and are therefore susceptible to being carried away at the expense of a smaller energy. They assumed that the material moisture content is made up of two major components. The first one is the bound moisture content corresponding to the water molecules strongly connected to the material molecules. The second one is the free moisture content that corresponds to the water molecules loosely connected to the material molecules. There is a certain conversion between these two forms of moisture molecules which could be modeled as a reversible reaction. Although bound water can only be converted into free water, the latter is the one that diffuses through the bulk of the material. The

proportion of free moisture content is initially very large, but as drying reaches its last stages it is the bound moisture molecules that form a majority of the water molecules, and therefore conversion between bound and free water controls the overall mass transfer phenomenon. In this way, mass transfer can be modeled so that it would include three basic transfer phenomena: external convection represented by the boundary layer mass transfer coefficient, free water diffusion represented by its corresponding diffusion coefficient, and conversion of bound water to free water represented by its appropriate kinetic constants. The total heat and mass transfer phenomenon can be expressed by the following equations:

$$\frac{\partial(\rho_B X_F)}{\partial t} = \nabla(\rho_B D \nabla X_F) + \rho_B r_B \tag{21}$$

$$-\frac{\partial X_B}{\partial t} = r_B \tag{22}$$

$$\frac{\partial(\rho_B h_S)}{\partial t} = h_H(T_A - T_S) - \Delta H_S h_M(a_{W_E} - a_W) \tag{23}$$

where X_B and X_F are the material bound and free moisture content, respectively, and r_B their corresponding conversion rate. The system state variables are the bound and free moisture content, and the solid-phase temperature. In equation (23) the solid-phase specific enthalpy will be computed using a mean material moisture content value throughout the sample, for a given time instant. The bound to free water conversion is assumed to follow a reversible path as modeled below:

$$r_B = k_1 X_B - k_2 X_F. \tag{24}$$

The corresponding boundary condition concerns only the free moisture content and can be expressed in the following form:

$$-\rho_B D \nabla X_F = h_M(a_{W_E} - a_W). \tag{25}$$

Furthermore, the material moisture content will be computed by means of its state components:

$$X_S = X_F + X_B. \tag{26}$$

The moisture diffusion coefficient is given by an Arrhenius-type of equation, expressing the corresponding temperature effect. This is the only state-dependent relation in the proposed model which is justified by the kinetic energy statement mentioned above:

$$D = D_0 \exp(-E_T/RT_S). \tag{27}$$

The sensitivity of model outputs to process parameter variations is included in Fig. 9. In this plot we examine certain effects of the kinetic constant values on the drying curve, that is to say how the material moisture content varies with time. The deviation of these curves was performed for process data similar to those of curve B in Fig. 6; external convection and internal diffusion of free water are both significant. In the case of curve A, the kinetic constant of bound water is infinite; no bound water is present. Diffusion is in control even in the last stages of drying, where the material moisture content decreases exponentially to its equilibrium value. Curve C represents the other extreme; no available free water. It is therefore an unrealistic case. Curve B lies somewhere in-between. All transfer mechanisms are presented. Mass transfer is sequentially controlled by convection, diffusion and conversion of bound to free water. It is obvious that by changing the values of the model parameters we can obtain nearly any kind of shape for the drying curve. The distributions of free and bound water are also included in Fig. 9. The case of free water resembles that water in curve B of Fig. 6, while bound water is always uniform throughout the material space at any time.

The Bayesian inference was again applied directly to all experimental points obtained for both materials using the model suggested above. The optimum model parameter values for heat and mass transfer coefficients are shown in Table 1. The individual residual distributions for both responses, along with their joint residual distribution for both materials, are presented in Figs. 4 and 5. In this case, both material temperature and moisture content distributions are of normal shape, with almost zero means and adequately small standard deviations. Regions B and C were shifted towards zero and the joint distribution of errors reveals the requested independent populations. Clearly, we can now explain the essense of these regions. Region A represents external convection, region B represents diffusion of free water molecules, and region C represents the conversion of bound to free molecules. In Figs. 4 and 5, the joint and individual distributions of the material moisture content and temperature residuals are presented for all models, giving us the full picture of how the model is improved through each step taken in the iterative procedure adopted. Similar conclusions can be derived by comparing the way that fitting is improved from the initially proposed model to the one obtained with the iterative procedure. In Fig. 10 we present the worst fit for the initial model and for both materials. The proposed model fits the experimental data almost exactly, while the intermediate one, involving the state-dependent moisture diffusivity, lies in-between.

The joint confidence regions of the Arrhenius equation parameters for the free-water diffusion coefficient for 90 and 95% levels of probability in the case of carrot are plotted in Fig. 11. The two parameters are strongly correlated. A wide range of several parameter values are equally probable, within a certain probability level, as for the optimum fit. Because of this correlation, we lack a precise estimation of the diffusion free energy, which is an important parameter cited in the literature. In the same plot the results of similar investigations are included. We note that, although there are significant differences between the actually calculated diffusion coefficient parameters, all

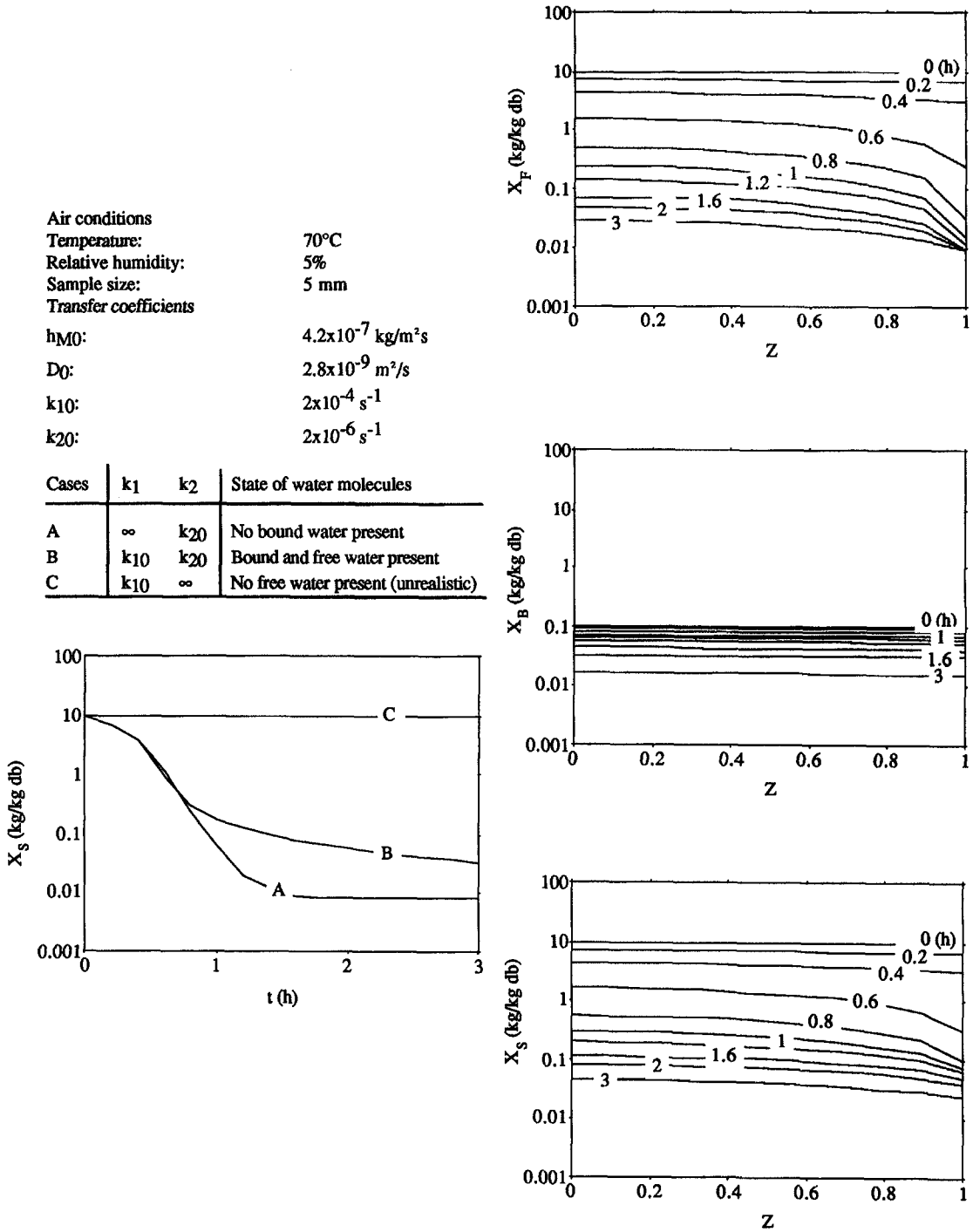

Fig. 9. Sensitivity analysis of the converted bound to free water drying model parameters.

of them, even the estimates of Kompany *et al.* [40], can be considered quite reasonable within the range of our experimental error.

CONCLUSION

Drying processes are characterized by numerous diversified heat and mass transfer mechanisms, and it is always difficult to discern between them when dealing with experimental data produced for various materials. A reliable model can be obtained when a sequential model building technique is used for the exploration of experimental drying data, using the material moisture content and temperature as process responses. An initial mathematical model is suitably tested by introducing the corresponding residuals

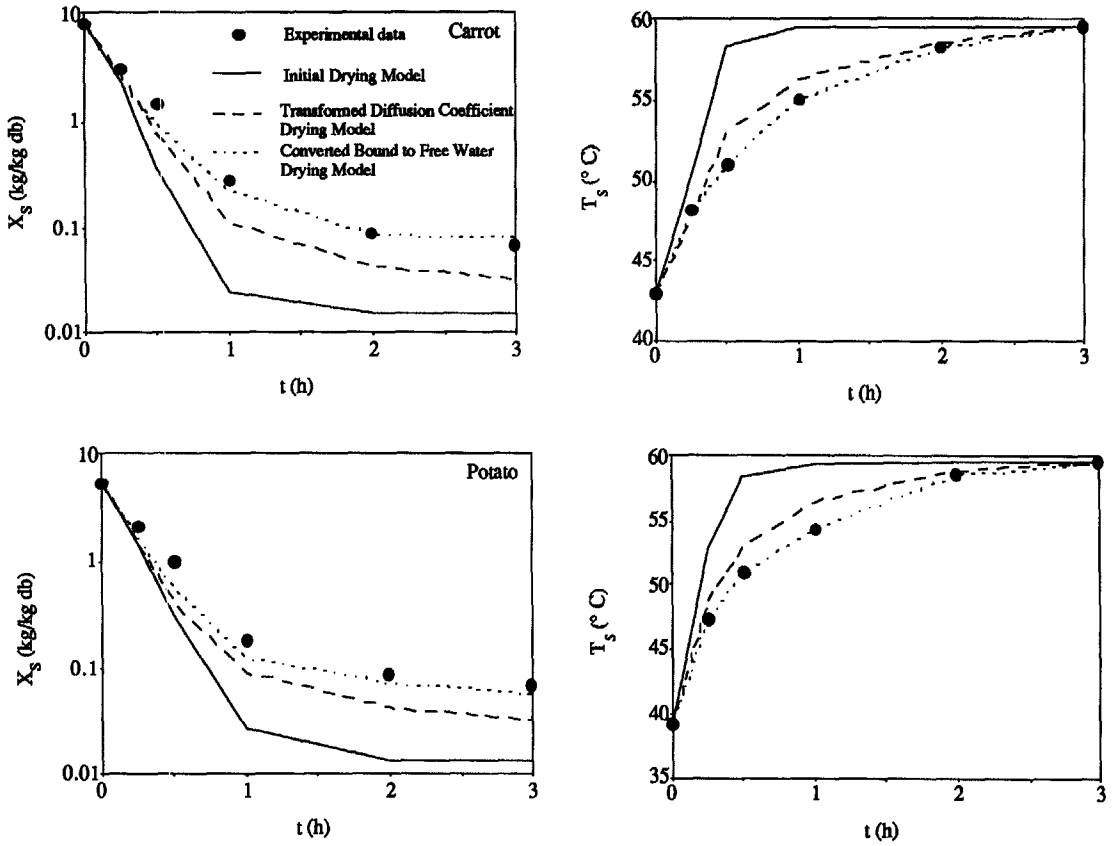

Fig. 10. Experimental and calculated points for the worst prediction by the initial model experiment for all models.

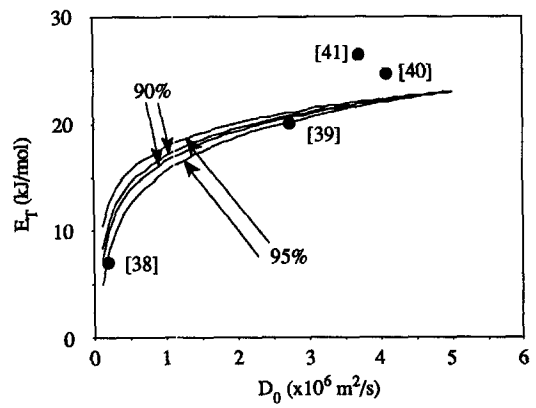

Fig. 11. Joint confidence regions of the Arrhenius equation parameters and comparison with corresponding values reported in the literature.

which are produced by fitting the model to experimental data using a multiresponse Bayesian parameter estimation technique. Guided by the model parameters' sensitivity to state variables, we are led by the tendencies in these residuals to improve or completely reconsider the transfer mechanisms involved. Modification of the proposed model stops when all observed tendencies are eliminated. This model building procedure can be used in the case of multiresponse drying data for vegetables using an initial model involving the effective mass diffusivity, the external mass transfer coefficient, the effective thermal conductivity and the external heat transfer coefficient as its parameters. It can be shown that mass transfer is controlled by external convection in the early stages, followed by water diffusion. When the drying reaches its last stages, the drying rate decreases dramatically due to the conversion of bound to free water molecules which controls the entire phenomenon. External heat convection is the only significant heat transfer mechanism found to exist for the experimental data used.

REFERENCES

1. G. E. P. Box and W. G. Hunter, A useful method for model building, *Technometrics* **4**, 301–318 (1962).
2. W. G. Hunter and R. Mezaki, A model building technique for chemical engineering kinetics, *A.I.Ch.E. Jl* **10**, 315–322 (1964).
3. E. R. Ziegel and J. W. Gorman, Kinetic modeling with multiresponse data, *Technometrics* **22**, 139–151 (1980).
4. G. N. Roman, M. J. Urbicain and E. Rotstein, Kinetics of the approach to sorptional equilibrium by a foodstuff, *A.I.Ch.E. Jl* **29**, 800–805 (1983).
5. M. A. Stanish, G. S. Schajer and F. Kayihan, A math-

ematical model of drying for hygroscopic porous media, *A.I.Ch.E. Jl* **32,** 1301–1311 (1986).
6. M. Fortes and M. R. Okos, Heat and mass transfer in hygroscopic capillary extruded products, *A.I.Ch.E. Jl* **27,** 255–262 (1981).
7. M. Ilic and I. W. Turner, Convective drying of a consolidated slab of wet porous material, *Int. J. Heat Mass Transfer* **32,** 2351–2362 (1989).
8. G. Arnaud and J. P. Fohr, Slow drying simulation in thick layers of granular products, *Int. J. Heat Mass Transfer* **31,** 2517–2525 (1988).
9. A. V. Luikov, Systems of differential equations of heat and mass transfer in capillary-porous bodies (review), *Int. J. Heat Mass Transfer* **18,** 1–14 (1975).
10. R. B. Keey and M. Suzuki, On the characteristic drying curve, *Int. J. Heat Mass Transfer* **17,** 1455–1464 (1974).
11. A. V. Luikov, T. L. Perelman, V. V. Levdansky, V. G. Leitsina and N. V. Pavlyukevich, Theoretical investigation of vapour transfer through a capillary-porous body, *Int. J. Heat Mass Transfer* **17,** 961–970 (1974).
12. G. E. P. Box and N. R. Draper, The Bayesian estimation of common parameters from several responses, *Biometrika* **52,** 355–365 (1965).
13. C. T. Kiranoudis, Z. B. Maroulis and D. Marinos-Kouris, Mass transfer model building in drying, *Drying Technol.* **11,** 1251–1270 (1993).
14. R. B. Keey, Theoretical foundations of drying technology. In *Advances in Drying* (Edited by A. S. Mujumdar), pp. 1–22. Hemisphere, New York (1980).
15. J. Van Brakel, Mass transfer in convective drying. In *Advances in Drying* (Edited by A. S. Mujumdar). Hemisphere, New York (1980).
16. J. Chirife, Fundamentals of the drying mechanism during air dehydration of foods. In *Advances in Drying* (Edited by A. S. Mujumdar), pp. 73–102. Hemisphere, New York (1983).
17. S. Bruin and K. C. A. M. Luyben, Drying of food materials: a review of recent developments. In *Advances in Drying* (Edited by A. S. Mujumdar), pp. 155–215. Hemisphere, New York (1980).
18. M. Fortes and M. R. Okos, Drying theories: their bases and limitations as applied to foods and grain. In *Advances in Drying* (Edited by A. S. Mujumdar), pp. 119–154. Hemisphere, New York (1980).
19. S. D. Holdsworth, Dehydration of food products. a review, *J. Food Technol.* **6,** 331–370 (1971).
20. J. L. Rossen and K. Hayakawa, Simultaneous heat and moisture transfer in dehydrated foods: a review of theoretical models, *A.I.Ch.E. Symp. Ser.* **73**(163), 71–81 (1977).
21. W. E. Van Arsdel, *Food Dehydration* I. *Principles*. AVI, Westport, CT (1963).
22. M. Karel, Properties controlling mass transfer in foods and related model systems. In *Theory, Determination and Control of Physical Properties of Food Materials* (Edited by C. Rha). Reide, Boston (1975).
23. K. W. Waananem, J. B. Litchfield and M. R. Okos, Classification of drying models for porous solids, *Drying Technol.* **11,** 1–40 (1993).
24. N. P. Zogzas, Z. B. Maroulis and D. Marinos-Kouris, Densities, shrinkage and porosity of some vegetables during air drying, *Drying Technol.* (1994).
25. C. T. Kiranoudis, Z. B. Maroulis, E. Tsami and D. Marinos-Kouris, Equilibrium moisture content and heat of desorption of some vegetables, *J. Food Engng* **20,** 55–74 (1993).
26. S. V. Patankar, *Numerical Heat Transfer and Fluid Flow*. Hemisphere, New York (1980).
27. B. Finlayson, *Non-linear Analysis in Chemical Engineering*. McGraw-Hill, New York (1980).
28. P. M. Reilly and H. Patino-Leal, A Bayesian study of the error-in-variables model, *Technometrics* **23,** 221–231 (1981).
29. W. E. Stewart, Multiresponse parameter estimation with a new and noninformative prior, *Biometrika* **74,** 557–562 (1987).
30. M. J. Box, N. R. Draper and W. G. Hunter, Missing values in multiresponse nonlinear model fitting, *Technometrics* **12,** 613–620 (1970).
31. W. E. Stewart and J. P. Sorensen, Bayesian estimation of common parameters from multiresponse data with missing observations, *Technometrics* **23,** 131–141 (1981).
32. J. V. Beck and K. J. Arnold, *Parameter Estimation in Engineering and Science*, p. 334. Wiley, New York (1977).
33. A. Mulet, A. Berna, M. Borras and F. Pinaga, Effect of air rate in carrot drying, *Drying Technol.* **5,** 245–258 (1987).
34. G. K. Vagenas and V. T. Karathanos, Prediction of moisture diffusivity in granular materials as a function of temperature and moisture content, *Biotechnol. Prog.* **7,** 419–428 (1991).
35. G. K. Vagenas and V. T. Karathanos, Prediction of the effective moisture diffusivity in gelatinised food system, *J. Food Engng* **18,** 159–179 (1993).
36. I.-W. Kim, M. J. Liebman and T. F. Edgar, Robust error-in-variables estimation using nonlinear programming techniques, *A.I.Ch.E. Jl* **36,** 985–993 (1990).
37. X. Xiong, G. Narsimhan and M. R. Okos, Effect of composition and pore stucture on binding energy and effective diffusivity of moisture in porous foods, *J. Food Engng* **15,** 187–208 (1991).
38. E. Kompany, J. Benchimol, K. Allof, B. Aiseba and J. M. Bouvier, Carrot dehydration for instant rehydration: dehydration kinetics and modelling, *Drying Technol.* **11,** 451–470 (1993).
39. J. J. Bimbenet, J. D. Dandin and E. Wolff, Air kinetics of biological particles. In *Drying* '85 (Edited by R. Toei and A. S. Mujumdar). Hemisphere, Washington, DC (1985).
40. A. Mullet, A. Berna and C. Rossello, Drying of carrots I. Drying models, *Drying Technol.* **7,** 537–557 (1989).
41. A. M. Sereno and G. L. Medeiros, A simplified model for the prediction of drying rates of foods, *J. Food Engng* **12,** 1–11 (1990).